



HAL
open science

Reconstruction of annual and seasonal variations in water temperature in the Haute-Dronne River of southwest France based on $\delta^{18}\text{O}$ records of freshwater pearl mussel shells (*M. margaritifera*), and its palaeoenvironmental implications

Emma Samin, Bruno Malaizé, Émilie P Dassié, Karine Charlier, Dominique Genty, Patricia Richard, Johan Vieira, Magalie Baudrimont

► To cite this version:

Emma Samin, Bruno Malaizé, Émilie P Dassié, Karine Charlier, Dominique Genty, et al.. Reconstruction of annual and seasonal variations in water temperature in the Haute-Dronne River of southwest France based on $\delta^{18}\text{O}$ records of freshwater pearl mussel shells (*M. margaritifera*), and its palaeoenvironmental implications. *Evolving Earth*, In press, pp.100012. 10.1016/j.eve.2023.100012 . hal-04234941

HAL Id: hal-04234941

<https://hal.science/hal-04234941>

Submitted on 10 Oct 2023

HAL is a multi-disciplinary open access archive for the deposit and dissemination of scientific research documents, whether they are published or not. The documents may come from teaching and research institutions in France or abroad, or from public or private research centers.

L'archive ouverte pluridisciplinaire **HAL**, est destinée au dépôt et à la diffusion de documents scientifiques de niveau recherche, publiés ou non, émanant des établissements d'enseignement et de recherche français ou étrangers, des laboratoires publics ou privés.

Journal Pre-proof

Reconstruction of annual and seasonal variations in water temperature in the Haute-Dronne River of southwest France based on $\delta^{18}\text{O}$ records of freshwater pearl mussel shells (*M. margaritifera*), and its palaeoenvironmental implications

Emma Samin, Bruno Malaizé, Émilie P. Dassié, Karine Charlier, Dominique Genty, Patricia Richard, Johan Vieira, Magalie Baudrimont

PII: S2950-1172(23)00012-2

DOI: <https://doi.org/10.1016/j.eve.2023.100012>

Reference: EVE 100012

To appear in: *Evolving Earth*

Received Date: 5 September 2023

Revised Date: 6 October 2023

Accepted Date: 6 October 2023

Please cite this article as: Samin, E., Malaizé, B., Dassié, É.P., Charlier, K., Genty, D., Richard, P., Vieira, J., Baudrimont, M., Reconstruction of annual and seasonal variations in water temperature in the Haute-Dronne River of southwest France based on $\delta^{18}\text{O}$ records of freshwater pearl mussel shells (*M. margaritifera*), and its palaeoenvironmental implications, *Evolving Earth* (2023), doi: <https://doi.org/10.1016/j.eve.2023.100012>.

This is a PDF file of an article that has undergone enhancements after acceptance, such as the addition of a cover page and metadata, and formatting for readability, but it is not yet the definitive version of record. This version will undergo additional copyediting, typesetting and review before it is published in its final form, but we are providing this version to give early visibility of the article. Please note that, during the production process, errors may be discovered which could affect the content, and all legal disclaimers that apply to the journal pertain.

© 2023 Published by Elsevier Ltd.



1 Reconstruction of annual and seasonal variations in
2 water temperature in the Haute-Dronne River of
3 southwest France based on $\delta^{18}\text{O}$ records of freshwater
4 pearl mussel shells (*M. margaritifera*), and its
5 palaeoenvironmental implications

6

7 Emma Samin¹, Bruno Malaizé¹, Émilie P. Dassié^{1*}, Karine Charlier¹, Dominique Genty¹, Patricia Richard²,
8 Johan Vieira³, Magalie Baudrimont¹

9 1. Environnements et Paléoenvironnements Océaniques et Continentaux (EPOC), Univ.
10 Bordeaux, CNRS, Bordeaux INP, EPOC, UMR 5805, F-33600 Pessac, France

11 2. Laboratoire des Sciences du Climat et de l'Environnement (LSCE/IPSL), CEA-CNRS UMR
12 8212-UVSQ, Université Paris-Saclay, 91191 Gif-sur-Yvette Cedex, France

13 3. Centre pour l'Aquaculture, la Pêche et l'Environnement de Nouvelle Aquitaine (CAPENA),
14 33470 Gujan-Mestras, France

15 * Corresponding author: emilie.dassie@u-bordeaux.fr

16

17 Keywords: *Margaritifera margaritifera*, shells, growth increments, oxygen isotopes,
18 temperature, freshwater

19

20 **Abstract**

21 The aragonitic shells of freshwater pearl mussels (*Margaritifera margaritifera*) contain annual growth
22 increments, whose composition reflect the geochemistry of the river water and bivalve metabolism.
23 The wide geographic distribution and the long lifespan of *M. margaritifera* coupled with a previously
24 established relationship between the $\delta^{18}\text{O}$ values of their shells and river temperature means this taxon
25 is a potentially important environmental archive; such freshwater proxies are currently limited in both
26 space and time. In this paper, we investigate the relationship between $\delta^{18}\text{O}$ values and both *in situ* and
27 modeled river temperature (2007 to 2015) for a population of *M. margaritifera* living in the Haute-
28 Dronne River (southwest France). Our $\delta^{18}\text{O}$ data permit the reconstruction of seasonal temperature
29 variations in the river. Sclerochronology reveals that shells have also record seasonal patterns and
30 produce winter growth increments, contrary to other investigations carried out on the same mussel
31 species from northern Europe where low winter temperatures (below 5°C) interrupt shell growth. The
32 presented calibration for *M. margaritifera* and host river temperature offers the potential for
33 reconstructing palaeoenvironmental conditions based on fossil specimens of the same species. Such

34 reconstructions may improve our understanding of past continental climate and help calibrate regional
35 palaeoclimate models.

36

37 1. Introduction

38 Recent climate changes are observed worldwide and request the interest of a large part of the scientific
39 community. Regional expressions of the observed global warming could lead to surprising
40 discrepancies regarding amplitudes and rate of changes. The paleoclimate community benefits from
41 multiple proxies extracted from different records coming from both oceanic and continental areas.
42 However, the limited number of continental proxies, in both space and time, encourages
43 paleoclimatologists to find new local archives to better constrain the regional-scale variability.

44 The freshwater pearl mussel *Margaritifera margaritifera* (Unionida) has been a subject of interest over
45 the last few decades as an indicator of the regional environmental conditions. *M. margaritifera* lives in
46 the northern hemisphere, particularly in western and central Europe, from the Iberian Peninsula to
47 Scandinavia. Under ideal living conditions, these mussels can reach an impressive lifespan, from a few
48 decades in Southern Europe to a nearly one hundred years in Scandinavia (Bauer, 1992; Mutvei and
49 Westermark, 2001; Schöne et al., 2004) making them a good paleoenvironmental archive.

50 *M. margaritifera* is classified as an “endangered” species on a global scale, and a “critically
51 endangered” species on a European scale by the International Union for Conservation of Nature (IUCN).
52 The global population of *M. margaritifera* has suffer a 90% loss during the 20th century. This loss can
53 be linked to both direct and indirect anthropogenic impacts, such as habitat degradation, pearl
54 harvesting, and the depletion of host fish populations (Bertucci et al., 2017, Baudrimont et al., 2020,
55 Life Haute-Dronne, 2021, Baudrimont, 2022). This species is very sensitive to its environment and
56 requires specific conditions such as shallow rivers with high flow velocities, cobble and gravel substrate,
57 low nutrient concentrations, and the presence of *Salmo trutta fario*, as its gills house larvae and allow
58 to disperse juveniles (Life final report, 2021, Bertucci et al., 2017).

59 The aragonitic shell of these mussels present annual growths increments, visible in both shell surface
60 and cross-sections. A growth slowdown or cessation is marked by the formation of darker layers (Jones
61 and Quitmyer, 1996) or thin opaque and organic scleroprotein-rich ridges (Geist et al., 2005). The
62 darker increments generally correspond, in most bivalve species, to winter shell accretion. Jones and
63 Quitmyer (1996) show, however significant latitudinal differences in the main accretion period,
64 sometimes even within the same species. In the majority of the studies, darker increments form when
65 river water temperature falls below a critical value during winter (designated as winter lines),
66 sometimes corresponding to an interruption in the shell growth. These disturbance lines are due to the
67 stress of the organism in its environment (Jones, 1983, Dunca et al., 2011, Dunca, 2014). Winter lines
68 make it possible to establish a sclerochronology for each individual and then determine their ages
69 (Mutvei and Westermark, 2001; Dunca et al., 2005; Helama et al., 2006). For *M. margaritifera*, the shell
70 growth interrupts when river temperature falls below 5°C, forming these denser and more resistant
71 lines, which delimit two summer growth increments (Dunca, 2014).

72 Various authors consider that water quality, pH, pollution, and nutrient availability could also influence
73 growth rates (Dunca et al., 2005; Dunca et al., 2011; Dunca, 2014). Helama et al. (2008) also note an
74 imprint of the lunar cycle on micro-growth patterns. However, specific dynamics of each population
75 make inter-comparisons complex (Dunca et al., 2011; Schöne et al., 2004). Besides those controversial
76 factors, the temperature appears to have an undeniable effect on the shell growth, as shown by the
77 distinction between winter lines and summer growth increments in marine and freshwater bivalve

78 shells (Dettman et al., 1998; Goodwin et al., 2001; Schöne et al., 2004; Dunca et al., 2005; Dunca et al.,
79 2011; Verdegaal et al., 2005; Versteegh et al., 2010a; Helama et al., 2014). In their study, Dunca et al.
80 (2005) showed that summer temperature variability can explain 35 % of annual growth variations.
81 Schöne et al. (2004) published a growth-temperature model deduced from increments thickness and
82 has demonstrated a similarity with paleo-temperatures deduced from regional dendrochronology
83 studies. Shell growth rate is therefore a valuable tool for reconstructing the river water paleo-
84 temperatures.

85 Furthermore, bivalves build their shell by drawing chemical elements that could be used as proxy of
86 environmental variability. Water $\delta^{18}\text{O}$ is known to be a good proxy of sources and amount of
87 precipitations. The isotopic signature of rainfall depends on the isotopic composition of the oceanic
88 evaporation area, and the distance between precipitation location and hydrological sources
89 (Dansgaard, 1964). Moreover, the fractionation between water and aragonite, depends on various
90 factors such as temperature (Grossman and Ku, 1985; Dettman et al., 1998) and precipitation regime
91 (Demény et al., 2012, Davis and Muehlenbachs, 2001). Recorded in carbonate shells, oxygen isotope
92 ratio become a valuable tool for paleoclimate reconstructions. Goodwin et al. (2001) and Izumida et al.
93 (2011) have thus conducted river paleo-temperatures reconstructions from bivalves' shells $\delta^{18}\text{O}$. Pfister
94 et al. (2018) and Schöne et al. (2020) have reconstructed rivers' $\delta^{18}\text{O}$ signal using both shells' isotopic
95 signature of this species and river temperature data. The aim of this study is to reconstruct river
96 temperature using both river and shells' isotopic signature .

97 France counts around a hundred thousand of *M. margaritifera* individuals, with the largest population
98 located in the Haute-Dronne River, Dordogne (SW of France, Figure 1) and reaching 15,000 specimens
99 according to a count carried out in 2003 by Patrice Cholet for the *Association Patrimoine Halieutique*
100 *Limousin Périgord*. The population of mussels living in the Haute-Dronne River thus represents 15% of
101 the national population; the species has disappeared from 60% of France's rivers in which it has been
102 identified at the beginning of the 20th century (Life Haute-Dronne, 2021). The Haute-Dronne River is
103 qualified as a remarkable area in France for the conservation of the species by the 'Museum National
104 d'Histoire Naturelle'. Thus, regarding the various hazards and ecological pressures on the species, the
105 population of Haute-Dronne River has been chosen for a special European Life + Nature program (2014
106 to 2021), to ensure the production and protection of this species (Life final report, 2021). This Life +
107 Nature program (2014-2021) aimed to rehabilitate the quality of the Haute-Dronne River to offer
108 adequate habitats to the population of pearl mussels and its host fish. During this project, territorial
109 planning has been developed to restore river natural stream. The *Salmo trutta fario* was granted
110 protected status, and an aquaculture farm has been created to support the population. In addition,
111 exceptional authorizations have been delivered to collect several specimens for shell and soft tissue
112 analyses to understand the interaction with the environment and the impact of potential pollution
113 (Bertucci et al., 2017, Baudrimont et al., 2020). The present study aims to re-use the collected shells,
114 given that specimens from this population are difficult to obtain due to their protected status, and to
115 exploit the potential of the species as paleo-marker. Indeed, shells of *M. margaritifera* are renowned
116 to be good archives due to (i) their long lifespan (ii) their quantifiable growth increments acting as
117 mussel's life chronology (iii) their ability to capture chemical elements from surrounding water,
118 especially oxygen isotopes whose proportion varies with seasonality, and (iv) their sentinel species
119 status, testifying to sustainable environmental conditions in the river during their life.

120 Shells collected as part of this project gave us the rare opportunity to conduct isotopic analyses on this
121 population. This study aims to evaluate the relationship between *M. margaritifera* shell $\delta^{18}\text{O}$ signature
122 and Haute-Dronne River temperature variations. This is a preliminary study including available regional
123 environmental data to assess the possibility of reconstructing the river temperature evolution through

124 *M. margaritifera* shells. The aim is to compare water temperature computed from aragonite oxygen
125 isotope fractionation with *in situ* and modeled river temperatures. Results from this study could
126 motivate further research with additional environmental data from river monitoring.

127 **2. Material and methods**

128 **2.1 Study area and instrumental datasets**

129 Empty shells have been collected on the riverbanks of the Haute-Dronne River in September 2015, near
130 the village of Saint-Saud Lacoussière, located in the northern part of Dordogne (SW-France, Figure 1),
131 authorization of sampling given by the DIREN (French Ministry of the Environment, Agreement
132 N°39/2016 in 2008). The area, located 200km from the Atlantic Ocean, is influenced by temperate
133 marine climate and Atlantic fluxes, with mild winters (average January-February-March = 6.5°C for
134 1984-2007) and relatively cool summers (July-August-September = 18.7°C) (Genty, 2008).

135 Over the last decades, the area climate parameters such as the air temperature (T_{air}), the amount of
136 precipitation (accuracy $\pm 0.2\text{mm}$), the rainfall isotopic signal ($\delta^{18}\text{O}_{\text{precip.}}$, measured using CO_2 equilibrium
137 on a Finnigan MAT 252, with an analytical error of $\pm 0.05 \text{‰}$), and the river temperature were
138 monitored (supp. mat. Table 1). For precipitation, both rainfall amount and isotopic signal have been
139 measured monthly since 1998, with rain gauges above the Villars cave, located twelve kilometres south
140 of the shell collection area (Figure 1). These data have been collected as part of other studies in the
141 area conducted on Villars cave's speleothems, renowned to be reference archives of regional
142 paleoclimate (Genty, 2008; Genty et al., 2014).

143 Local river temperatures have been measured punctually from 2006 to 2019 by the *Laboratoire*
144 *d'Analyse et de Recherche de Dordogne (LDAR24)* but unfortunately without a regular sampling
145 interval. Therefore, there is no monthly record available for the river temperature. However, a monthly
146 air temperature record since 1950 exists for the area, provided by the European Environment Agency
147 (E-OBS gridded dataset, https://surfobs.climate.copernicus.eu/dataaccess/access_eobs.php, last
148 access spring 2023). By comparing river and air temperature datasets, we found a significant linear
149 correlation ($r^2 = 0.81$, $p\text{-value} < 0.01$) between both signals (Figure 2). We therefore decided to derive
150 river temperatures from air temperatures and create a monthly modelled river temperature dataset
151 (T_{Dronne}) (supp. mat. Table 2). For the purpose of our study, we have arbitrarily created seasonally
152 resolved datasets for which seasons are defined as December-January-February interval for winter,
153 March-April-May interval for spring, June-July-August interval for summer, and September-October-
154 November interval for autumn.

155 **2.2 Shells collection and preparation**

156 Four *M. margaritifera* shells have been selected for our study, referenced as S144, S185, S187, and
157 S194. Given their position and preservation state, the mussels were dead a few weeks before being
158 collected, probably killed by a predator (nutria, Pichon, 2017).

159 The shells were embedded at the EPOC Laboratory (Environnements et Paléoenvironnements
160 Océaniques et Continentaux, UMR5805, University of Bordeaux, France) in Epoxy resin Araldite 2020
161 as recommended by Schöne et al. (2017) to avoid geochemical contamination between carbonates and
162 Epoxy. Three-to-four-millimetre width sections were cut, cross-sectioning the shell in the direction of
163 minimum length, from the umbo (juvenile material) to the ventral margin (recent material) (Figure 3).
164 Shells' cross-section pictures have been taken using a stereo microscope Kern OZO553 coupled with a
165 camera Kern ODC825 supported by Microscope VIS[®] software.

166 **2.3 Micro-drilling and oxygen stable isotope analyses**

167 Shell sampling has been carried out at LSCE laboratory (Laboratoire des Sciences du Climat et de
 168 l'Environnement, UMR8212, Gif-sur-Yvette, France) using a Micromill PXC14 (New wave Research, with
 169 Komet drills H99 104 008) coupled with MEO[®] software. The furrows have been drilled into the
 170 prismatic layer of the shells, following the inclination of the dark and light increments (Figure 4). We
 171 configured the device to drill a furrow with a depth of 100 μm , across the whole width of the prismatic
 172 layer. The furrow width is estimated around 250 μm from the camera images. Due to the size of the
 173 drill bit, we were able to only sample one or two furrows on each increment (two to four values per
 174 year), which allowed to reach bi-annual resolution (Figure 4). Between 50 and 150 μg of powder have
 175 been collected for each furrow.

176 Powder samples have been analysed by Isotope Ratio Mass Spectrometry (IRMS) at the EPOC
 177 laboratory. Samples were dissolved with an acid solution of 103% H_3PO_4 at 90°C in a Kiel IV-carbonate
 178 sample preparation device linked to the IRMS. The $\delta^{18}\text{O}$ signature of the generated CO_2 gas was
 179 analysed in a Mat253 ThermoFisher IRMS. $\delta^{18}\text{O}$ values are missing for some increments because we
 180 were not able to collect enough powder. The international standard NBS19, referenced to Vienna Pee
 181 Dee Belemnite (VPDB) has been analysed in the same conditions as the shells' samples. Over the
 182 duration of the shells' analyses, the average standard deviation of the NBS19 was 0.03‰ (N= 23).

183 **2.4 Shell curvature correction**

184 To be able to visually compare growth increments aspect and spatial variation of stable isotopes values,
 185 we corrected the shell curvature (Figure 5). We pointed the XY coordinates of each furrow on cross-
 186 section pictures with ImageJ[®] software, to measure segment lengths between nearby points and thus
 187 sample spacing. We summed segments to compute the distance of each sample from the ventral
 188 margin. For the same purpose, cross-section pictures were adjusted to correct the shell curvature by
 189 flattening the prismatic layer along the horizontal axis. These two stages allowed us to directly compare
 190 shells pictures and growth increments with isotopic values variation, aligned on a horizontal axis (Figure
 191 5).

192 **3. Results**

193 **3.1 Shells' increments and $\delta^{18}\text{O}$ variability**

194 The shells' pictures taken with the stereo microscope show dark and light growth increments, probably
 195 related to seasonal accretion (Figure 4 and Figure 5). This assumption is supported by the difference
 196 between the isotopic values of dark and light increments. As shown in Figure 5, shells' $\delta^{18}\text{O}$ signatures
 197 present a range of variability similar to each other's, with values ranging between -3.7 and -5.4‰.
 198 Maxima occur for dark increments and minima for the light ones. The amplitude of the $\delta^{18}\text{O}$ signal
 199 reduces towards the ventral margin, especially visible for S144 and S185. Increment widths also
 200 decrease throughout mussel life, with larger increments corresponding to the first years of the
 201 organism life.

202 **3.2 Seasonal variation**

203 *3.2.1 Age Model*

204 To built our age model, we counted annual layers in both the corrected images and isotopic
 205 measurement records; the highest $\delta^{18}\text{O}$ values corresponding to darker increments, (Figure 5).
 206 Assuming that mussels died shortly before being collected in September 2015, the ventral margin is
 207 used as a time marker (summer period). Therefore, we used light and dark increments, also
 208 corresponding to $\delta^{18}\text{O}$ minima and maxima values, as a seasonal signal with a combination of two
 209 successive increments (one light with one dark) corresponding to one year of accretion, to count

210 backward from 2015. Using this method, we counted around eight to ten years for each. This age
 211 corresponds to a minimum age since there was a loss of the early stages of life due to erosion of the
 212 umbo. Once established, those age models allowed us to compare individuals' shell $\delta^{18}\text{O}$ records to
 213 one another.

214 While for most of the records, high $\delta^{18}\text{O}$ values correspond to dark increments, and low $\delta^{18}\text{O}$ values to
 215 light increments, some measurements do not fit this pattern. Regarding points closed to increment
 216 transitions, we can suspect that the constrain on the sampling resolution may be the source of this
 217 discrepancy. However, we cannot assume this hypothesis for points located in the centre of increments,
 218 as for the fifth light increment from the ventral margin, with high values comparable to values related
 219 to dark increments, and corresponding to summer 2010 in all shells (Figure 5).

220 3.2.2 Water temperature computation from shells' $\delta^{18}\text{O}$ signature

221 In 1985, Grossman and Ku published an equation describing the fractionation and the incorporation of
 222 oxygen isotopes in aragonite deposition, as a function of the temperature and the $\delta^{18}\text{O}$ composition of
 223 the surrounding water. The equation corrected by Dettman et al. (1998) is as follows (Equation 1):

$$224 \quad 1000 * \ln(\alpha) = 2.559(10^6 * T_{w(K)}^{-2}) + 0.715 \quad \text{Eq. (1)}$$

225 Where $T_{w(K)}$ is the river temperature, expressed in Kelvin, and α is the fractionation between water
 226 and aragonite, computed as:

$$227 \quad \alpha_{arag.}^{water} = \frac{1000 + \delta^{18}\text{O}_{arag. (SMOW)}}{1000 + \delta^{18}\text{O}_{water (SMOW)}} \quad \text{Eq. (2)}$$

228 To convert our isotopic values relative to the Vienna Pee Dee Belemnite (VPDB) reference to values
 229 relative to the Vienna Standard Mean Ocean Water (VSMOW), we applied the Eq. (3) from Gonfiantini
 230 et al. (1995):

$$231 \quad \delta^{18}\text{O}_{arag. (SMOW)} = 1.03091(1000 + \delta^{18}\text{O}_{arag. (VPDB)}) - 1000 \quad \text{Eq. (3)}$$

232 Unfortunately, $\delta^{18}\text{O}_{water}$ has never been measured in the river. To conduct our study, we must assume
 233 that the $\delta^{18}\text{O}_{water}$ of the Haute-Dronne River might be close to the rainfall isotopic composition
 234 ($\delta^{18}\text{O}_{precip.}$) measured at Villars' cave. We are conscious of the uncertainties linked with this hypothesis,
 235 which constitutes a weakness in this study. This work is a preliminary study that use previously collected
 236 specimens to look at their potential for environmental reconstructions in the region. Therefore, we can
 237 only reconstruct semi quantitative temperature timeseries and we will therefore solely focus our
 238 interpretation on temperature variability. Meanwhile we think that this assumption remains realistic,
 239 considering the relatively small size of the Haute-Dronne River watershed (Figure 1) and the
 240 metamorphic and granitic riverbed which limits water infiltration (D. Genty, per communication). Both
 241 factors, added to *M. margaritifera* host rivers characteristics (low depth, high velocities), suppose a fast
 242 response time of river runoff to rainfall, with efficient water drainage on the watershed.

243 Chronology based on the distinction of dark-light increments gives a nearly seasonal resolution for our
 244 shells' $\delta^{18}\text{O}$ records. Both seasonal shells' $\delta^{18}\text{O}$ values and precipitation are implemented into Eq. (2) to
 245 compute theoretical river temperatures records (Eq. (1)) deduced from each shell (T_w^{S144} , T_w^{S185} , T_w^{S187} ,
 246 T_w^{S194}). The average reconstructed temperature record T_w shows a similar range of variability with T_{Dronne}
 247 for the 2007-2015 time period (Figure 6).

248 Figure 6 presents the equation components, with shells' $\delta^{18}\text{O}$ (Fig 6a), river's $\delta^{18}\text{O}$ derived from
 249 $\delta^{18}\text{O}_{precip}$ (Fig 6b), and both river-modelled and reconstructed water temperatures from the two

250 previous parameters (Fig 6c). $\delta^{18}\text{O}_{\text{precip}}$ maxima and shells' $\delta^{18}\text{O}$ minima are in phase with temperature
251 maxima.

252

253 4. Discussion

254 4.1 Shells' $\delta^{18}\text{O}$ variability

255 In our study, the succession of light and dark increments, suggested that this population is undergoing
256 continuous shell growth with winter material deposition, contrary to northern populations whose
257 growth interrupts for water coldest temperatures (Mutvei and Westermark, 2001; Schöne et al.,
258 2004b; Schöne et al., 2005; Dunca et al., 2005; Helama et al., 2006; Helama et al., 2008; Dunca et al.,
259 2011; Dunca, 2014; Helama et al., 2014; Pfister et al., 2018; Schöne et al., 2020). Dark increments, with
260 higher $\delta^{18}\text{O}$ values, might be related to winter growth. Indeed, previous authors have demonstrated
261 that bivalves' aragonite precipitation near winter lines incorporates less negative $\delta^{18}\text{O}$ values than for
262 the constitution of summer growth increments (Goodwin et al., 2001; Schöne et al., 2005; Izumida et
263 al., 2011; Pfister et al., 2018; Schöne et al., 2020). According to *in situ* and modelled data, the river
264 temperature rarely falls below the mussels' minimum growth temperature (5°C according to Dunca,
265 2014), preserving them from complete growth cessation during this cold season. Furthermore,
266 population monitoring in Portugal, living in relatively warmer waters, also clearly shows continuous
267 growth in winter (Joaquim Reis, University of Lisbon, Marine and Environmental Sciences Centre, per
268 communication). The Haute-Dronne *M. margaritifera* population is therefore capable of recording
269 both summer and winter variability, reinforcing its potential as a climate proxy.

270 The Haute-Dronne temperatures reconstructed from *M. margaritifera* shells are in good agreement
271 with *in situ* and modelled temperature data. This procedure has already been carried out in other
272 regions on marine (*Chione cortezi*) and freshwater (*Hyriopsis* sp.) aragonitic shells by Goodwin et al.
273 (2001,2003) and Izumida et al. (2011) respectively and has given reliable river paleo-temperature
274 reconstructions. Here we do not pretend to compute extreme river temperature, conscious of the
275 uncertainties linked to our study, (i) the use of average values of water isotopic composition and mixed
276 material for each increment due to furrows width), (ii) the use of river $\delta^{18}\text{O}$ values derived from
277 precipitation $\delta^{18}\text{O}$. However, we clearly show the possibility of reconstructing the annual river
278 temperature cycle.

279 Regarding increment widths, the observed narrowing near the ventral margin agrees with previous
280 studies (Hastie et al., 2000; Helama et al., 2008; Dunca et al., 2011; Dunca,2014). The authors presented
281 variable growth curves between populations, all showing significant thinning of increments after the
282 first years of mussel life due to growth slowdown.

283 In our study, aragonite $\delta^{18}\text{O}$ values are higher than what was found in previous studies on *M.*
284 *margaritifera*. For populations in Sweden, Schöne et al. (2005, 2020) showed values ranging from -9.32
285 to -13.89‰. For populations in Luxembourg, Pfister et al. (2018) presented values between -6 and -
286 7‰ depending on seasonality. On Unionids bivalves in Rhine and Meuse, Verdegaal et al. (2005) and
287 Versteegh et al. (2010a, 2010b) determined mean values of -9‰ and -6.5‰, respectively. This feature
288 is in accordance with the isotopic gradient of meteoric waters observed over Europe (Langebroek et
289 al., 2011). Moreover, compared to northern sites, the population from the Haute-Dronne River is far
290 away from glacier meltwater influence and under the fluxes of Atlantic moisture with rare solid
291 precipitation (snow) which could explain the observed less negative values (Dansgaard, 1964).

292 4.2 Water and shells' $\delta^{18}\text{O}$ contributions to temperature reconstruction

293 To determine the weighting of each factor ($\delta^{18}\text{O}_{\text{water}}$ and shells' $\delta^{18}\text{O}$) on the river temperature
 294 reconstruction, we first computed theoretical water temperature only from shells' $\delta^{18}\text{O}$ values by
 295 fixing the $\delta^{18}\text{O}_{\text{water}}$ to its mean value to negate the influence of its variations. The seasonal amplitude
 296 of this newly shells' $\delta^{18}\text{O}$ -derived river temperature ($T_{w\text{-arag}}$), represents 30% of the total signal
 297 amplitude (Figure 7), and is significantly correlated to *in situ* and modelled river temperatures
 298 (Pearson linear correlation, $R^2 = 0.62$, p-value = 0.0003). Additionally, $T_{w\text{-precip}}$ determined secondly by
 299 fixing shells' $\delta^{18}\text{O}$ to its mean value, presents a seasonal amplitude close to the total signal amplitude
 300 (80%). Mean T_w , $T_{w\text{-precip}}$, and $T_{w\text{-arg}}$ are not statistically different (p-value = 0.97 with Kruskal-Wallis test).

301 We can conclude that the shells' $\delta^{18}\text{O}$ signature would not be sufficient in itself to reconstruct the full
 302 amplitude of T_w , but this proxy provides a valuable information on river mean temperature and
 303 seasonality. Shells' $\delta^{18}\text{O}$ can therefore be a powerful tool to reconstruct river temperature variability
 304 even if reconstructed signal is an attenuated one.

305 4.3 Remarkable summers

306 4.3.1 Summer 2010

307 A plateau is observed for summer 2010 in all selected shells' $\delta^{18}\text{O}$ measurements (Figure 6). As the
 308 plateau is observed for the four records, we can exclude the hypothesis of mussels' independent
 309 behaviour. This event might refer to a local or regional climatic influence. However, no anomaly can be
 310 detected neither on both rainfall amount and $\delta^{18}\text{O}_{\text{precip}}$ signal (Figures 7 and 6) nor in river *in situ* and
 311 modelled temperatures (Figure 6). We suppose that another environmental factor, not related to the
 312 river temperature (T_{Dronne}) or $\delta^{18}\text{O}_{\text{precip}}$ signal, could be responsible for this anomaly. It would be
 313 interesting to complete this study with additional measurements such as trace elements analyses that
 314 are known proxies of environmental changes.

315 The reconstructed temperature T_w for summer 2010 is only slightly lower than mean reconstructed
 316 temperature values over the entire length of the record, showing that the unexpectedly high $\delta^{18}\text{O}$
 317 values induce only a minor effect on the river temperature amplitude reconstruction. This is certainly
 318 due to the limited (around 30%) influence of shells' $\delta^{18}\text{O}$ variability, as explained in Section 4.2.
 319 Likewise, winter 2009 and 2012 also show the dominance of the $\delta^{18}\text{O}_{\text{water}}$ factor in reconstructed
 320 temperature signal amplitude (Figure 6).

321 4.3.2 Summer 2011

322 A large discrepancy can be observed between reconstructed and measured temperature data during
 323 summer 2011 (Figure 6). T_w is computed from T_w^{S144} , T_w^{S185} , T_w^{S187} , and T_w^{S194} and a sampling offset
 324 repeated on the four shells is unlikely. The observed deviation could be explained by the approximation
 325 of the river water $\delta^{18}\text{O}$ signal, which we have associated with $\delta^{18}\text{O}_{\text{precip}}$, due to the lack of data on the
 326 river. Nevertheless, regarding the amount of precipitation measured at Villars' cave (Genty, per
 327 communication), a significant rainfall deficit is observed in 2011 (Figure 8). A deficit in rainwater supply
 328 to the river would logically involve a river $\delta^{18}\text{O}$ signal linked with other sources further upstream or
 329 underground. Moreover, considering the large weight of this factor in water temperature
 330 reconstruction, an incorrect estimation of the water $\delta^{18}\text{O}$ value could fully explain the discrepancy.
 331 Unfortunately, further data on the river are lacking to test this hypothesis. Complementary shells trace
 332 elements analyses might also help constrain this deviation.

333 5. Conclusion

334 This study aimed to assess the potential of *M. Margaritifera* shells from the Haute-Dronne River
 335 population as a proxy for regional paleo-environmental reconstructions. We show that this population

336 provides an annual record of river conditions, covering each season (winter included) suggesting a
337 nearly continuous growth over the year. Additionally, $\delta^{18}\text{O}$ recorded in shells allowed to reconstruct
338 river paleo-temperatures during the organism's life from 2007 to 2015. We use rainfall isotopic d18O
339 composition to derived river d18O values since no measurements of river $\delta^{18}\text{O}$ are available for the
340 time interval covered by our shells. While this method seems convincing, it might be interesting to
341 measure the annual variability of this parameter in the river for future studies. Meanwhile this work
342 clearly demonstrates the possibility of reconstructing the seasonal variability of the Haute-Dronne
343 River temperature by using the isotopic signature of *M. margaritifera* shells regarding the clear
344 difference of $\delta^{18}\text{O}$ values between dark and light growth increments. According to these promising
345 results, we could now consider conducting a similar study on longer time scales with older or fossilized
346 shells, as some authors have done with fossilized freshwater bivalves shells in other regions to
347 reconstruct precipitations (Davis and Muehlenbachs, 2001, with *Margaritifera facalta*), global
348 environmental changes (Demény et al., 2012, with *Unio* sp.) and river $\delta^{18}\text{O}$ signals (Versteegh et al.,
349 2010b, with *Unio* sp.). To fine-tune our study on this population, we could carry out trace elements
350 analyses to better understand river's physicochemical cycles and physiological process. *M.*
351 *margaritifera* shells are certainly inadequate to fully reconstitute the amplitude of temperature
352 seasonal variations, but still provide a valuable water temperature average and constitute good river
353 archives when no information exists on watercourses. Moreover, these shells can highlight multi
354 decadal trends, recorded throughout the mussels' long life. We could thus consider recovering
355 temperature trends over the last decades with an annual resolution, which is remarkable for
356 continental archives under temperate climate.

357

358

359

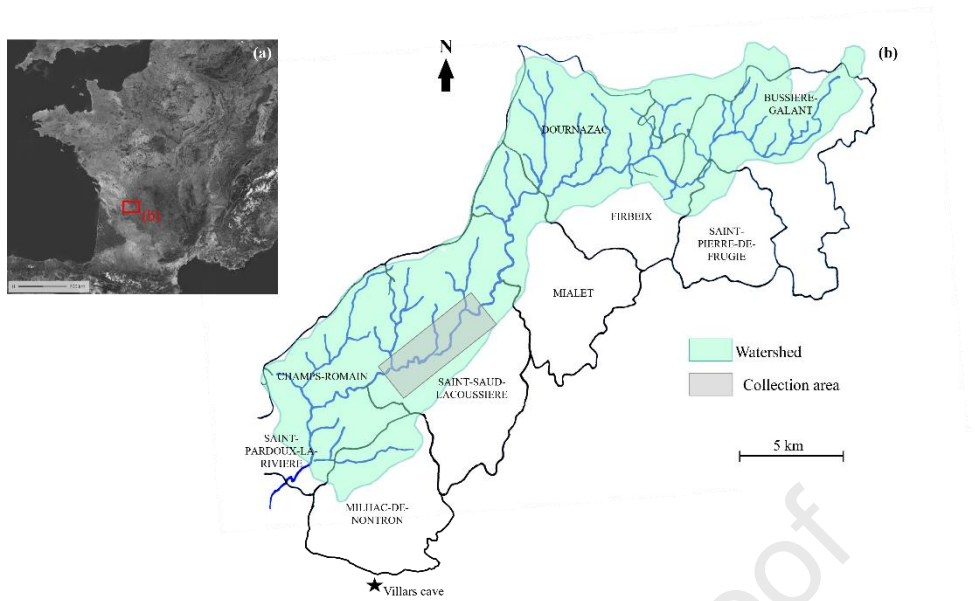
360 **Acknowledgments** The authors benefit from the financial support of the "Département de Sciences de
361 l'Environnement de l'Université de Bordeaux – Projets émergents", as well as the Life + Nature
362 European program (LIFE13 NAT/FR/000506). We acknowledge the E-OBS dataset from the EU-FP6
363 project UERRA (<https://www.uerra.eu>) and the Copernicus Climate Change Service, and the data
364 providers in the ECA&D project (<https://www.ecad.eu>). We acknowledge the Laboratoire d'Analyse et
365 de Recherche de Dordogne (LRAR24) for Haute-Dronne temperature measurements. We would like to
366 thank Margaux Saint-George in EPOC laboratory for technical support (thin sections preparation) and
367 Bénédicte Minster for $\delta^{18}\text{O}_{\text{precip}}$ analyses in LSCE laboratory. Villars rainfall isotopic measurements are
368 now part of the national isotopic rainfall observatory SNO RENOIR (coord. E. Gibert, GEOPS, Univ. Paris-
369 Saclay). We also had valuable discussion with Joaquim Reis.

370 **References**

- 371 Baudrimont M. (2022). Préservation de *Margaritifera margaritifera* et restauration de la continuité
 372 écologique de la Haute Dronne. Volet 3 : Amélioration des connaissances sur la biologie et
 373 l'écotoxicologie de la Petite Mulette. Rapport scientifique final AEAG, projet LIFE+ Nature LIFE13
 374 NAT/FR/000506, p. 39.
- 375 Baudrimont, M., Gonzalez, P., Mesmer-Dudons, N., & Legeay, A. (2020). Sensitivity to cadmium of the
 376 endangered freshwater pearl mussel *Margaritifera margaritifera* from the Dronne River (France):
 377 experimental exposure. *Environmental Science and Pollution Research*, 27, 3715-3725.
- 378
 379 Bauer, G. (1992). Variation in the life span and size of the freshwater pearl mussel. *Journal of animal*
 380 *ecology*, 425-436.
- 381
 382 Bertucci, A., Pierron, F., Thébault, J., Klopp, C., Bellec, J., Gonzalez, P., & Baudrimont, M. (2017).
 383 Transcriptomic responses of the endangered freshwater mussel *Margaritifera margaritifera* to trace
 384 metal contamination in the Dronne River, France. *Environmental Science and Pollution Research*, 24,
 385 27145-27159.
- 386
 387 Cornes, R., G. van der Schrier, E.J.M. van den Besselaar, and P.D. Jones. 2018: An Ensemble Version of
 388 the E-OBS Temperature and Precipitation Datasets, *J. Geophys. Res. Atmos.*, **123**.
 389 doi:10.1029/2017JD028200
- 390
 391 Dansgaard, W. (1964). Stable isotopes in precipitation. *tellus*, 16(4), 436-468.
- 392
 393 Davis, L. G., & Muehlenbachs, K. (2001). A Late Pleistocene to Holocene record of precipitation
 394 reflected in *Margaritifera falcata* shell $\delta^{18}\text{O}$ from three archaeological sites in the lower Salmon River
 395 Canyon, Idaho. *Journal of Archaeological Science*, 28(3), 291-303.
- 396
 397 Demény, A., Schöll-Barna, G., Fórizs, I., Osán, J., Sümegi, P., & Bajnóczi, B. (2012). Stable isotope
 398 compositions and trace element concentrations in freshwater bivalve shells (*Unio* sp.) as indicators of
 399 environmental changes at Tiszapüspöki, eastern Hungary. *Central European Geology*, 55(4), 441-460.
- 400
 401 Dettman, D. L., Reische, A. K., & Lohmann, K. C. (1999). Controls on the stable isotope composition of
 402 seasonal growth bands in aragonitic fresh-water bivalves (Unionidae). *Geochimica et Cosmochimica*
 403 *Acta*, 63(7-8), 1049-1057.
- 404
 405 Dunca, E., Schöne, B. R., & Mutvei, H. (2005). Freshwater bivalves tell of past climates: But how clearly
 406 do shells from polluted rivers speak?. *Palaeogeography, Palaeoclimatology, Palaeoecology*, 228(1-2),
 407 43-57.
- 408
 409 Dunca, E., Söderberg, H., & Norrgrann, O. (2011). Shell growth and age determination in the freshwater
 410 pearl mussel *Margaritifera margaritifera* in Sweden: natural versus limed streams. *Ferrantia*, 64, 48-
 411 58.
- 412
 413 Dunca, E. (2014). Growth and chemical analyses of freshwater pearl mussel, *Margaritifera*
 414 *margaritifera*, shells from Haukåselva river, Norway.
- 415
 416 Geist, J., Auerswald, K., & Boom, A. (2005). Stable carbon isotopes in freshwater mussel shells:
 417 environmental record or marker for metabolic activity?. *Geochimica et Cosmochimica Acta*, 69(14),
 418 3545-3554.

- 419
420 Genty, D. (2008). Palaeoclimate research in Villars Cave (Dordogne, SW-France). *International Journal*
421 *of Speleology*, 37(3), 173-191.
422
- 423 Genty, D., Labuhn, I., Hoffmann, G., Danis, P. A., Mestre, O., Bourges, F., ... & Minster, B. (2014). Rainfall
424 and cave water isotopic relationships in two South-France sites. *Geochimica et Cosmochimica Acta*,
425 131, 323-343.
426
- 427 Gonfiantini, R., Stichler, W., & Rozanski, K. (1995). *Standards and intercomparison materials distributed*
428 *by the International Atomic Energy Agency for stable isotope measurements* (No. IAEA-TECDOC--825).
429
- 430 Goodwin, D. H., Flessa, K. W., Schone, B. R., & Dettman, D. L. (2001). Cross-calibration of daily growth
431 increments, stable isotope variation, and temperature in the Gulf of California bivalve mollusk *Chione*
432 *cortezii*: implications for paleoenvironmental analysis. *Palaaios*, 16(4), 387-398.
433
- 434 Goodwin, D. H., Schone, B. R., & Dettman, D. L. (2003). Resolution and fidelity of oxygen isotopes as
435 paleotemperature proxies in bivalve mollusk shells: models and observations. *Palaaios*, 18(2), 110-125.
436
- 437 Grossman, E. L., & Ku, T. L. (1986). Oxygen and carbon isotope fractionation in biogenic aragonite:
438 temperature effects. *Chemical Geology: Isotope Geoscience Section*, 59, 59-74.
439
- 440 Helama, S., Schöne, B. R., Black, B. A., & Dunca, E. (2006). Constructing long-term proxy series for
441 aquatic environments with absolute dating control using a sclerochronological approach: introduction
442 and advanced applications. *Marine and Freshwater Research*, 57(6), 591-599.
443
- 444 Helama, S., & Valovirta, I. (2008). Ontogenetic morphometrics of individual freshwater pearl mussels
445 (*Margaritifera margaritifera* (L.)) reconstructed from geometric conchology and trigonometric
446 sclerochronology. *Hydrobiologia*, 610, 43-53.
447
- 448 Helama, S., & Valovirta, I. (2014). An autoecological study of annual shell growth increments in
449 *Margaritifera margaritifera* from Lapland, Subarctic Finland. *Memoir of the Fukui Prefectural Dinosaur*
450 *Museum*, 13, 25-35.
451
- 452 Izumida, H., Yoshimura, T., Suzuki, A., Nakashima, R., Ishimura, T., Yasuhara, M., ... & Kawahata, H.
453 (2011). Biological and water chemistry controls on Sr/Ca, Ba/Ca, Mg/Ca and $\delta^{18}\text{O}$ profiles in freshwater
454 pearl mussel *Hyriopsis* sp. *Palaeogeography, Palaeoclimatology, Palaeoecology*, 309(3-4), 298-308.
455
- 456 Jones, D. S. (1983). Sclerochronology: reading the record of the molluscan shell: annual growth
457 increments in the shells of bivalve molluscs record marine climatic changes and reveal surprising
458 longevity. *American Scientist*, 71(4), 384-391.
459
- 460 Jones, D. S., & Quitmyer, I. R. (1996). Marking time with bivalve shells: oxygen isotopes and season of
461 annual increment formation. *Palaaios*, 340-346.
462
- 463 Life Haute-Dronne, programme LIFE 13 NAT/FR/000506, rapport final, août 2021, 212 p.
- 464 Langebroek, P. M., Werner, M., & Lohmann, G. (2011). Climate information imprinted in oxygen-
465 isotopic composition of precipitation in Europe. *Earth and Planetary Science Letters*, 311(1-2), 144-
466 154.
467

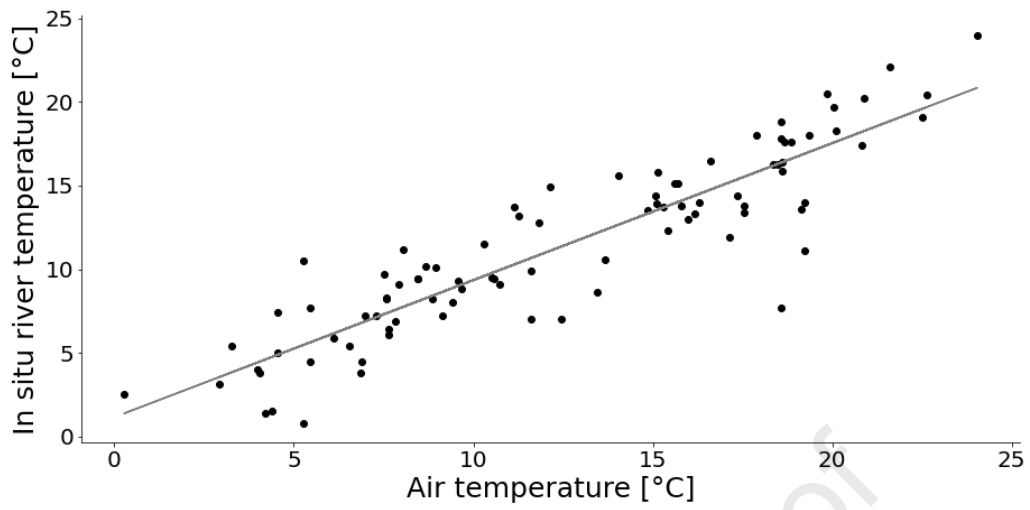
- 468 Millot, R., Petelet-Giraud, E., Guerrot, C., & Négrel, P. (2010). Multi-isotopic composition ($\delta^7\text{Li}$ – $\delta^{11}\text{B}$ –
 469 δD – $\delta^{18}\text{O}$) of rainwaters in France: Origin and spatio-temporal characterization. *Applied Geochemistry*,
 470 25(10), 1510-1524.
- 471
 472 Mutvei, H., & Westermark, T. (2001). How environmental information can be obtained from Naiad
 473 shells. *Ecology and evolution of the freshwater mussels Unionoida*, 367-379.
- 474
 475 Nyström, J., Lindh, U., Dunca, E., & Mutvei, H. (1995). A study of *M. margaritifera* shells from the River
 476 Pauliströmsån, S. Sweden. *Nuclear Instruments and Methods in Physics Research Section B: Beam
 477 Interactions with Materials and Atoms*, 104(1-4), 612-618.
- 478
 479 Pfister, L., Thielen, F., Deloule, E., Valle, N., Lentzen, E., Grave, C., ... & McDonnell, J. J. (2018).
 480 Freshwater pearl mussels as a stream water stable isotope recorder. *Ecohydrology*, 11(7), e2007.
- 481
 482 Pichon, C. 2017. Un cas de prédation de la moule perlière *Margaritifera margaritifera* (Linnaeus 1758)
 483 sur le bassin versant de la Dronne en Dordogne, MalaCo, 13 : 22-24.
- 484
 485 Schöne, B. R., Castro, A. D. F., Fiebig, J., Houk, S. D., Oschmann, W., & Kröncke, I. (2004a). Sea surface
 486 water temperatures over the period 1884–1983 reconstructed from oxygen isotope ratios of a bivalve
 487 mollusk shell (*Arctica islandica*, southern North Sea). *Palaeogeography, Palaeoclimatology,
 488 Palaeoecology*, 212(3-4), 215-232.
- 489
 490 Schöne, B. R., Dunca, E., Mutvei, H., & Norlund, U. (2004b). A 217-year record of summer air
 491 temperature reconstructed from freshwater pearl mussels (*M. margaritifera*, Sweden). *Quaternary
 492 Science Reviews*, 23(16-17), 1803-1816.
- 493
 494 Schöne, B. R., Dunca, E., Mutvei, H., Baier, S., & Fiebig, J. (2005). Scandinavian climate since the late
 495 18th century reconstructed from shells of bivalve mollusks. *ZEITSCHRIFT-DEUTSCHEN GESELLSCHAFT
 496 FÜR GEOWISSENSCHAFTEN*, 156(4), 501.
- 497
 498 Schöne, B. R., Schmitt, K., & Maus, M. (2017). Effects of sample pretreatment and external
 499 contamination on bivalve shell and Carrara marble $\delta^{18}\text{O}$ and $\delta^{13}\text{C}$ signatures. *Palaeogeography,
 500 Palaeoclimatology, Palaeoecology*, 484, 22-32.
- 501
 502 Schöne, B. R., Meret, A. E., Baier, S. M., Fiebig, J., Esper, J., McDonnell, J., & Pfister, L. (2020).
 503 Freshwater pearl mussels from northern Sweden serve as long-term, high-resolution stream water
 504 isotope recorders. *Hydrology and earth system sciences*, 24(2), 673-696.
- 505
 506 Verdegaal, S., Troelstra, S. R., Beets, C. J., & Vonhof, H. B. (2005). Stable isotopic records in unionid
 507 shells as a paleoenvironmental tool. *Netherlands Journal of Geosciences*, 84(4), 403-408.
- 508
 509 Versteegh, E. A., Vonhof, H. B., Troelstra, S. R., Kaandorp, R. J., & Kroon, D. (2010a). Seasonally resolved
 510 growth of freshwater bivalves determined by oxygen and carbon isotope shell chemistry.
 511 *Geochemistry, Geophysics, Geosystems*, 11(8).
- 512
 513 Versteegh, E. A. A., Vonhof, H. B., Troelstra, S. R., & Kroon, D. (2010b). A molluscan perspective on
 514 hydrological cycle dynamics in northwestern Europe. *Netherlands Journal of Geosciences*, 89(1), 51-60.
- 515



516

517 *Figure 1 – Maps of the location of the *M. margaritifera* population (a) Map of France (source: <https://www.geoportail.gouv.fr/>)*
 518 *with study area location in SW of France (b) Map of the Haute-Dronne river (blue) and corresponding watershed (green)*
 519 *(source: Life final report, modified). Shells have been collected close to the village of Saint-Saud Lacoussière, in the area in*
 520 *grey. The Villars cave where have been collected precipitation data is located a few kilometers southern the collection area.*

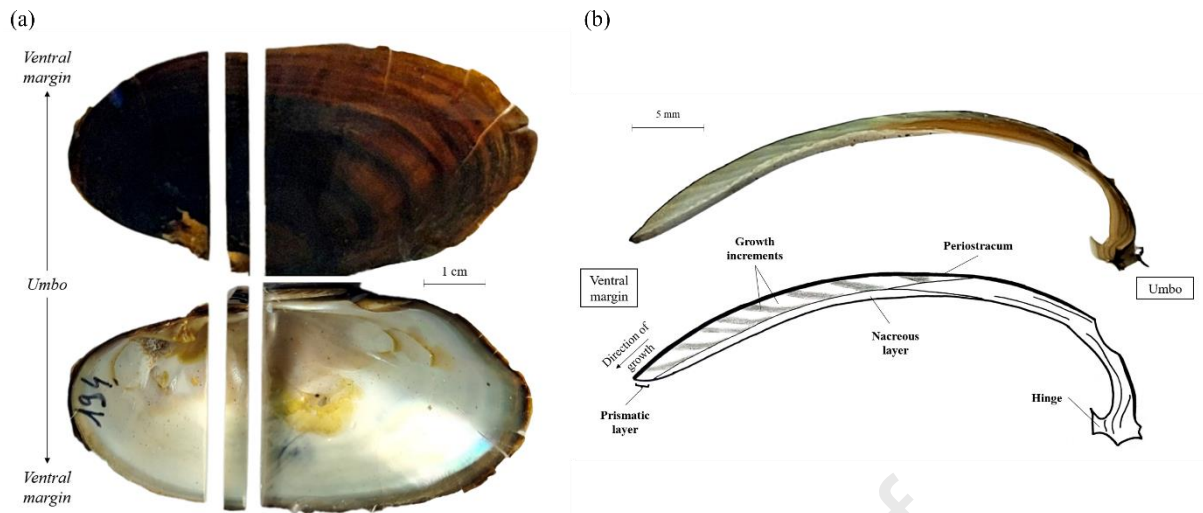
521



522

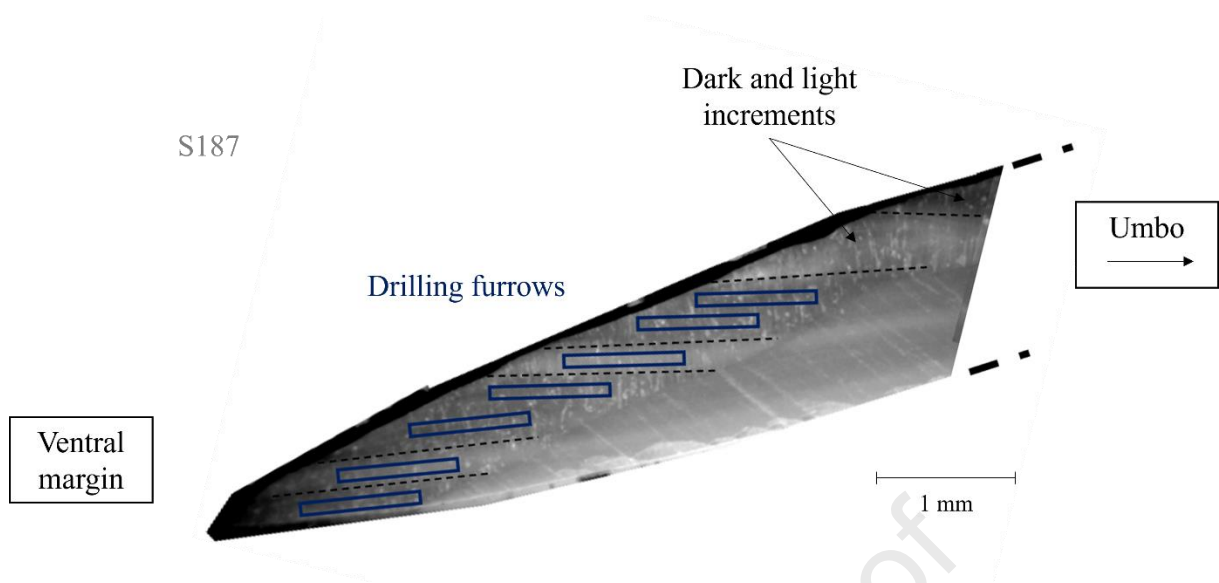
523 *Figure 2 - Comparison between in situ river temperature measurements (provided by the Laboratoire d'Analyse et de*
524 *Recherche de Dordogne LDAR24) and corresponding air temperature at Villars (provided by the European Environment*
525 *Agency). A linear correlation is found between the two parameters (Pearson correlation, $R^2 = 0.81$, $p\text{-value} < 0.01$).*

526



527

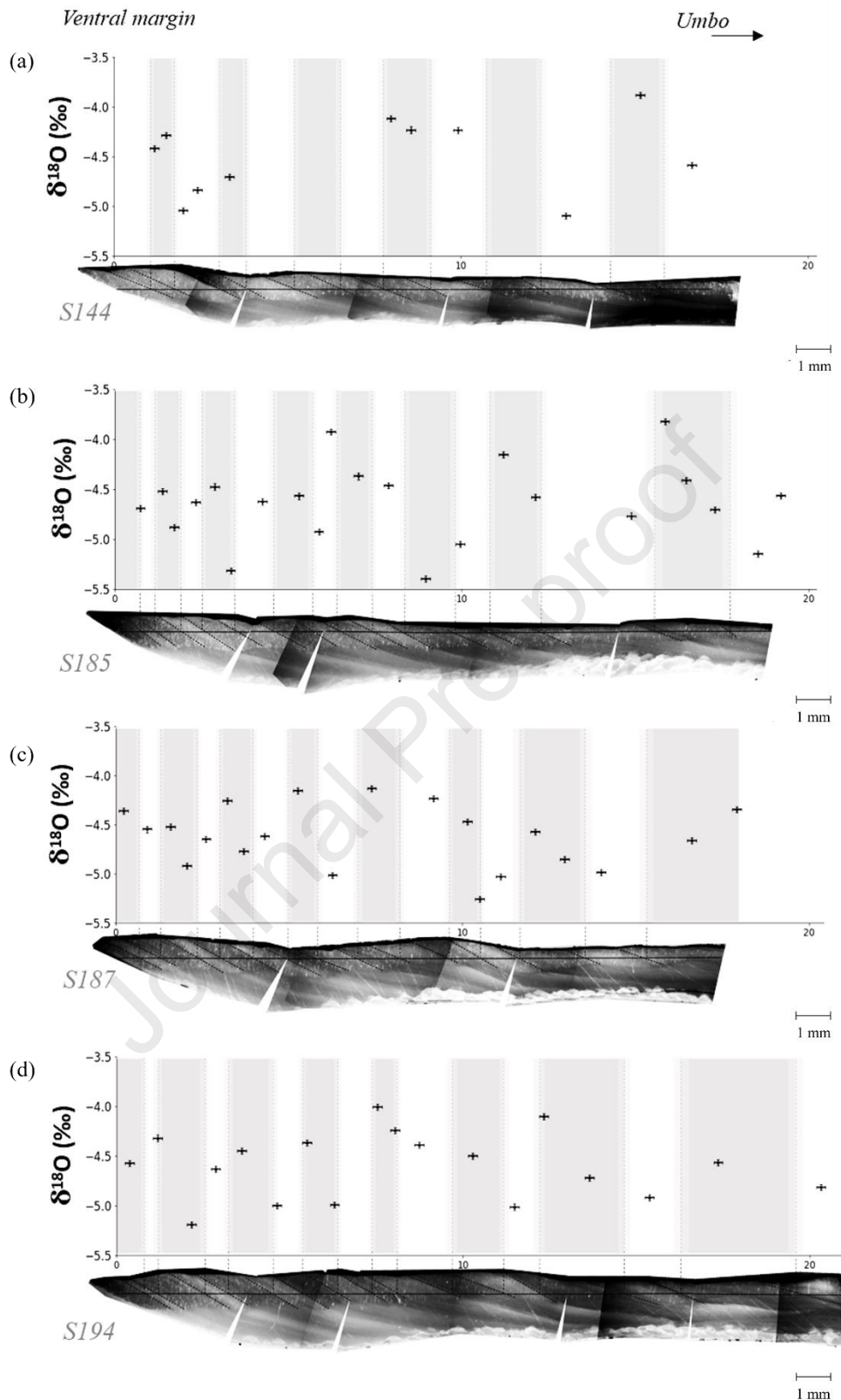
528 *Figure 3 – M. Margaritifera shells (a) Outer and inner sides of shells, with visible increments on the outer side. Shells cross-*
 529 *sections have been cut from the umbo to the ventral margin, perpendicular to growth increments, in the direction of minimum*
 530 *length. (b) Cross-section scanner imagery (up) and schematic reproduction of main structures (down), including dark and light*
 531 *growth increments in the prismatic layer.*



532

533 *Figure 4 – Part shells' dark and light growth increments sampling, located on the ventral margin. Drilling paths are limited to*
 534 *the prismatic layer and are chosen in regards to the distinction of dark and light increments on stereo microscope pictures, by*
 535 *accentuating contrasts. One or two furrows are drilled on each depending on increments width.*

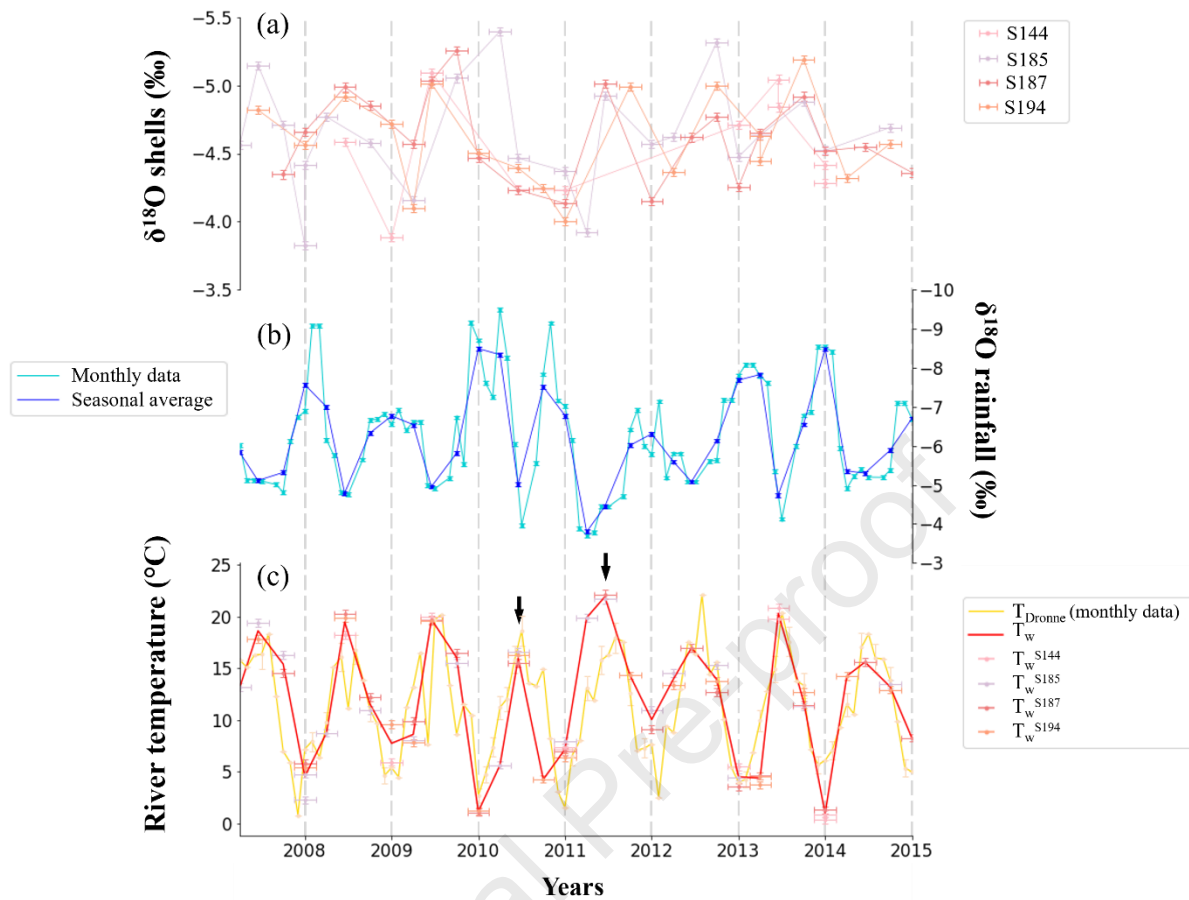
536



537

538 Figure 5 – $\delta^{18}\text{O}$ records for the four selected shells (a) S144 (b) S185 (c) S187 (d) S194. Measurements have been carried out
 539 with an IRMS device on powder samples collected for each furrow drilled in growth increments. Dark and light increments
 540 were differentiated by dark and light gradients on charts. Stereo microscope pictures have been planarized along the charts'
 541 x-axis to enable the comparison between shells' structures and $\delta^{18}\text{O}$ values.

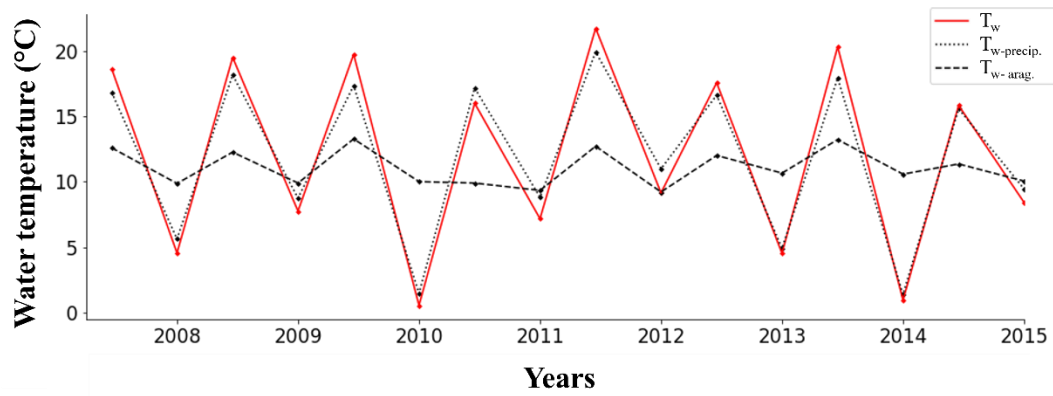
542



543

544 Figure 6 – (a) Shells' $\delta^{18}\text{O}$ records aligned on age model (reversed y-axis) (b) $\delta^{18}\text{O}$ record of rainfall, monthly measured above
 545 the Villars cave (light blue), close to the mussels' living area (data provided by D. Genty) (reversed y-axis). The seasonal average
 546 has been computed (dark blue) as DJF = winter, MAM = spring, JJA = summer, SON = autumn (c) Monthly T_{Dronne} record (yellow)
 547 compared with reconstructed temperature average T_w (red), computed from Grossman and Ku equation (1986), corrected by
 548 Dettman et al. (1999). Grey dashed lines indicate winters and black arrows point to remarkable summers.

549

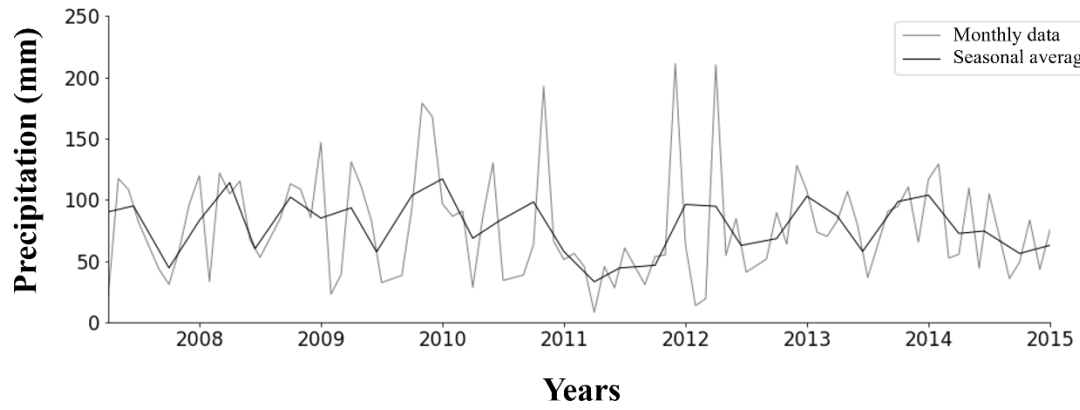


550

551 *Figure 7 – Theoretical winter and summer temperature reconstructions only considering rainfall $\delta^{18}O$ variation ($T_{w-precip}$ thin*
 552 *black dashed line) and shells $\delta^{18}O$ variation (T_{w-arag} bold black dashed line). Only winter and summer T_w are represented to*
 553 *compare $T_{w-precip}$ and T_{w-arag} amplitudes with the expected signal.*

554

Journal Pre-proof



555

556 *Figure 8 – Monthly record of precipitation amount measured above the Villars cave (grey) (data provided by D. Genty), and*
557 *seasonal average (black). The year 2011 shows an annual rainfall deficit compared to the other years over the considered*
558 *period in the region.*

559

Journal Pre-proof

560 Supplements

561 *Table 1 – Monthly amount of precipitations (mm) and isotopic composition $\delta^{18}O_{precip.}$ (‰) measured above the Villars cave*
 562 *from 2007 to 2015 (data provided by D. Genty). Monthly modeled air temperature at Villars T_{air} (°C) (data provided by E-OBS,*
 563 *https://surfobs.climate.copernicus.eu/dataaccess/access_eobs.php)*

Date	Precipitation ± 0.2 [mm]	Villars rainfall $\delta^{18}O \pm$ 0.05 [‰]	Villars air temperature [°C]
15/01/2007	87.5	-6.41	6.85
15/02/2007	141.6	-6.41	8.44
15/03/2007	132.3	-6.34	8.46
15/04/2007	20.8	-6.02	15.15
15/05/2007	117.3	-5.13	15.71
15/06/2007	108.3	-5.13	18.36
15/07/2007	81.6	-5.09	18.54
15/08/2007			18.57
15/09/2007	43.5	-5.01	15.43
15/10/2007	30.9	-4.81	12.46
15/11/2007	58.6	-6.13	6.10
15/12/2007	96.3	-6.73	5.28
15/01/2008	119.6	-6.89	6.98
15/02/2008	33.2	-9.08	8.27
15/03/2008	121.8	-9.08	7.63
15/04/2008	104.8	-6.15	10.50
15/05/2008	115.3	-5.76	15.62
15/06/2008	67.1	-4.81	18.24
15/07/2008	53.0	-4.76	19.22
15/08/2008			19.10
15/09/2008	84.9	-5.65	15.10
15/10/2008	113.0	-6.65	12.04
15/11/2008	108.5	-6.68	7.52
15/12/2008	85.3	-6.82	4.27
15/01/2009	146.7	-6.55	3.27
15/02/2009	23.0	-6.93	5.45
15/03/2009	38.9	-6.40	8.06
15/04/2009	130.8	-6.62	11.27
15/05/2009	110.4	-6.62	16.60
15/06/2009	82.6	-5.00	18.59
15/07/2009	32.4	-4.90	20.04
15/08/2009			20.90
15/09/2009	38.3	-5.18	17.55
15/10/2009	93.8	-6.73	13.44
15/11/2009	178.8	-5.53	10.30
15/12/2009	167.9	-9.16	5.26
15/01/2010	96.7	-8.71	1.89
15/02/2010	86.5	-7.61	4.37
15/03/2010	90.7	-7.26	7.61
15/04/2010	28.4	-9.49	12.29
15/05/2010	86.5	-8.27	13.29

15/06/2010	130.1	-6.04	17.93
15/07/2010	34.2	-3.97	21.31
15/08/2010			19.13
15/09/2010	38.5	-5.55	16.18
15/10/2010	63.5	-7.83	12.13
15/11/2010	192.6	-9.15	7.58
15/12/2010	66.0	-7.16	2.92
15/01/2011	51.1	-7.01	4.40
15/02/2011	56.2	-6.15	6.55
15/03/2011	45.6	-3.89	9.43
15/04/2011	8.1	-3.71	14.57
15/05/2011	45.5	-3.78	17.13
15/06/2011	28.1	-4.44	17.87
15/07/2011	60.6	-4.43	18.48
15/08/2011			20.50
15/09/2011	30.8	-4.71	18.86
15/10/2011	53.6	-6.42	13.98
15/11/2011	55.0	-6.91	11.61
15/12/2011	211.1	-5.99	7.50
15/01/2012	63.6	-5.79	5.44
15/02/2012	13.6	-7.14	0.27
15/03/2012	19.3	-5.18	10.57
15/04/2012	210.1	-5.80	9.68
15/05/2012	54.6	-5.80	15.99
15/06/2012	84.6	-5.08	18.68
16/07/2012	40.9	-5.08	18.60
16/08/2012	14.4		21.62
15/09/2012	51.6	-5.61	17.35
16/10/2012	89.5	-5.63	14.04
15/11/2012	63.7	-7.17	8.95
16/12/2012	128.0	-7.17	6.54
16/01/2013	107.0	-7.80	3.99
13/02/2013	73.5	-8.08	3.78
16/03/2013	70.1	-8.08	7.82
15/04/2013	83.0	-7.80	10.72
16/05/2013	106.9	-7.61	11.84
15/06/2013	79.2	-5.34	16.81
16/07/2013	36.5	-4.12	22.65
16/08/2013	50.3		20.05
15/09/2013	90.6	-5.99	17.55
16/10/2013	94.6	-6.78	14.91
15/11/2013	110.5	-6.87	7.31
16/12/2013	65.4	-8.53	5.51
16/01/2014	116.7	-8.53	7.63
13/02/2014	129.2	-8.42	7.20
16/03/2014	52.4	-5.94	9.59
15/04/2014	55.5	-4.90	12.64
16/05/2014	109.6	-5.22	13.67

15/06/2014	44.1	-5.40	19.39
16/07/2014	104.8	-5.20	20.10
16/08/2014	72.1		18.10
15/09/2014	35.6	-5.19	18.61
16/10/2014	49.3	-5.38	15.50
15/11/2014	83.5	-7.09	11.60
16/12/2014	43.1	-7.09	5.15
16/01/2015	75.6	-6.70	4.56
13/02/2015	69.8	-6.31	4.29
16/03/2015	48.0	-5.67	9.14
15/04/2015	47.7	-4.66	13.00
16/05/2015	46.8	-5.56	15.31
15/06/2015	52.3	-4.43	20.23
16/07/2015	9.2	-5.48	22.52
16/08/2015	101.3		20.91
15/09/2015	62.0	-5.08	15.80
16/10/2015	57.5	-5.08	12.18
15/11/2015	51.2	-4.81	10.74
16/12/2015	10.5	-3.28	8.72

564

565

566 *Table 2 - Monthly Haute-Dronne temperature T_{Dronne} from 2007 to 2015, including in situ measurements (provided by the*
567 *Laboratoire d'Analyse et de Recherche de Dordogne) and additional values modeled from the linear relationship between the*
568 *air temperature at Villars (provided by E-OBS, https://surfobs.climate.copernicus.eu/dataaccess/access_eobs.php) and the*
569 *river temperature. The uncertainty on the in situ river temperatures are not provided and consequently considered as*
570 *negligible. The uncertainty on the modeled temperatures is computed from the model parameters.*

Date	River temperature [°C]	Uncertainty	Data type
01/2007	3.8	0.0	<i>in situ</i>
02/2007	9.4	0.0	<i>in situ</i>
03/2007	9.4	0.0	<i>in situ</i>
04/2007	15.8	0.0	<i>in situ</i>
05/2007	15.1	0.0	<i>in situ</i>
06/2007	16.3	0.0	<i>in situ</i>
07/2007	16.3	1.4	modeled
08/2007	18.3	0.0	<i>in situ</i>
09/2007	12.3	0.0	<i>in situ</i>
10/2007	7.0	0.0	<i>in situ</i>
11/2007	5.9	0.0	<i>in situ</i>
12/2007	0.8	0.0	<i>in situ</i>
01/2008	7.2	0.0	<i>in situ</i>
02/2008	7.9	0.9	modeled
03/2008	6.4	0.0	<i>in situ</i>
04/2008	9.8	1.0	modeled

05/2008	15.1	0.0	<i>in situ</i>
06/2008	16.1	1.4	modeled
07/2008	11.1	0.0	<i>in situ</i>
08/2008	16.8	1.4	modeled
09/2008	13.9	0.0	<i>in situ</i>
10/2008	11.0	1.1	modeled
11/2008	9.7	0.0	<i>in situ</i>
12/2008	4.7	0.8	modeled
01/2009	5.4	0.0	<i>in situ</i>
02/2009	4.5	0.0	<i>in situ</i>
03/2009	11.2	0.0	<i>in situ</i>
04/2009	13.2	0.0	<i>in situ</i>
05/2009	16.5	0.0	<i>in situ</i>
06/2009	7.7	0.0	<i>in situ</i>
07/2009	19.7	0.0	<i>in situ</i>
08/2009	20.2	0.0	<i>in situ</i>
09/2009	13.4	0.0	<i>in situ</i>
10/2009	8.6	0.0	<i>in situ</i>
11/2009	11.5	0.0	<i>in situ</i>
12/2009	10.5	0.0	<i>in situ</i>
01/2010	2.7	0.7	modeled
02/2010	4.7	0.8	modeled
03/2010	7.4	0.9	modeled
04/2010	11.2	1.1	modeled
05/2010	12.0	1.1	modeled
06/2010	15.8	1.3	modeled
07/2010	18.6	1.5	modeled
08/2010	13.6	0.0	<i>in situ</i>
09/2010	13.3	0.0	<i>in situ</i>
10/2010	14.9	0.0	<i>in situ</i>
11/2010	8.3	0.0	<i>in situ</i>
12/2010	3.1	0.0	<i>in situ</i>
01/2011	1.5	0.0	<i>in situ</i>
02/2011	6.5	0.9	modeled
03/2011	8.0	0.0	<i>in situ</i>
04/2011	13.1	1.2	modeled
05/2011	11.9	0.0	<i>in situ</i>
06/2011	15.8	1.3	modeled
07/2011	16.3	0.0	<i>in situ</i>
08/2011	18.0	1.4	modeled

09/2011	17.6	0.0	<i>in situ</i>
10/2011	12.6	1.2	modeled
11/2011	7.1	0.0	<i>in situ</i>
12/2011	7.3	0.9	modeled
01/2012	7.7	0.0	<i>in situ</i>
02/2012	2.5	0.0	<i>in situ</i>
03/2012	9.4	0.0	<i>in situ</i>
04/2012	8.8	0.0	<i>in situ</i>
05/2012	13.0	0.0	<i>in situ</i>
06/2012	17.6	0.0	<i>in situ</i>
07/2012	16.4	0.0	<i>in situ</i>
08/2012	22.1	0.0	<i>in situ</i>
09/2012	14.4	0.0	<i>in situ</i>
10/2012	15.6	0.0	<i>in situ</i>
11/2012	10.1	0.0	<i>in situ</i>
12/2012	5.4	0.0	<i>in situ</i>
01/2013	4.0	0.0	<i>in situ</i>
02/2013	4.2	0.7	modeled
03/2013	6.9	0.0	<i>in situ</i>
04/2013	9.9	1.0	modeled
05/2013	12.8	0.0	<i>in situ</i>
06/2013	14.9	1.3	modeled
07/2013	20.4	0.0	<i>in situ</i>
08/2013	17.6	1.4	modeled
09/2013	13.8	0.0	<i>in situ</i>
10/2013	13.4	1.2	modeled
11/2013	7.2	0.0	<i>in situ</i>
12/2013	5.7	0.8	modeled
01/2014	6.1	0.0	<i>in situ</i>
02/2014	7.1	0.9	modeled
03/2014	9.3	0.0	<i>in situ</i>
04/2014	11.5	1.1	modeled
05/2014	10.6	0.0	<i>in situ</i>
06/2014	17.0	1.4	modeled
07/2014	18.3	0.0	<i>in situ</i>
08/2014	16.0	1.3	modeled
09/2014	15.9	0.0	<i>in situ</i>
10/2014	13.9	1.2	modeled
11/2014	9.9	0.0	<i>in situ</i>
12/2014	5.4	0.8	modeled

01/2015	5.0	0.0	<i>in situ</i>
02/2015	4.7	0.8	modeled
03/2015	7.2	0.0	<i>in situ</i>
04/2015	11.8	1.1	modeled
05/2015	13.7	0.0	<i>in situ</i>
06/2015	17.7	1.4	modeled
07/2015	19.1	0.0	<i>in situ</i>
08/2015	18.3	1.5	modeled
09/2015	13.8	0.0	<i>in situ</i>
10/2015	11.1	1.1	modeled
11/2015	9.1	0.0	<i>in situ</i>
12/2015	8.3	1.0	modeled

571

572

Journal Pre-proof

Declaration of interests

The authors declare that they have no known competing financial interests or personal relationships that could have appeared to influence the work reported in this paper.

The authors declare the following financial interests/personal relationships which may be considered as potential competing interests:

Bruno Malaize reports financial support was provided by University of Bordeaux.

Journal Pre-proof